

## DSC study on the motor protein myosin in fibre system

T. Dergez<sup>a,\*</sup>, F. Könczöl<sup>b</sup>, M. Kiss<sup>a</sup>, N. Farkas<sup>a</sup>

<sup>a</sup> Institute of Bioanalysis, University of Pécs, School of Medicine, Pécs H-7624, Szigeti str. 12, Hungary

<sup>b</sup> Institute of Forensic Medicine, University of Pécs, School of Medicine,  
Pécs H-7624, Szigeti str. 12, Hungary

Available online 22 March 2006

### Abstract

We have examined by DSC the complexes of myosin with actin in fibre system in the absence of nucleotides and the intermediate state of ATP hydrolysis by mimicking stable complex with myosin and ADP and beryllium fluoride in muscle fibres. Comparing the DSC results with other structural analogues of phosphate  $P_i$  leads the conclusion that the AM.ADP.BeF<sub>x</sub> complex favours the AM.ADP.P<sub>i</sub> complex in fibre system. The deconvolution of DSC scans resulted in four transitions, the first three transition temperatures were almost independent of the intermediate state of the muscle, the last transition temperature was shifted to higher temperature, depending on the actual intermediate states of ATP hydrolysis. In AM.ADP.V<sub>i</sub> state the transition temperature at the second and third transitions (actin binding domain and myosin rod) varied only slightly, whereas the last one (the fourth transition) shifted markedly to higher temperature depending on the ternary complex, e.g. in case of ADP plus BeF<sub>x</sub> it was 77.7 °C, the highest value in weakly binding state of myosin to actin. The sum of calorimetric enthalpies of the first and last curves was practically constant, but their fractions depended on the state of the muscle. In strongly binding state of myosin to actin (rigor, ADP state) the fraction of the first transition was much larger, than the last one, whereas in weakly binding state of myosin to actin, the fraction of the first transition decreased at the expense of the last one. It supports also the view that these transitions are parts of the same portion of the myosin molecule.

© 2006 Published by Elsevier B.V.

**Keywords:** Myosin; Actin; Motor protein; DSC

### 1. Introduction

Muscle contraction and other events of cell motility are based on the cyclic interaction of the head portion of myosin with actin during the myosin-catalysed ATP hydrolysis. The hydrolysis of ATP that produces the AM.ADP.P<sub>i</sub> complex (A denotes actin and M stands for myosin) and the protein-bound ADP and P<sub>i</sub> is a rapid process, therefore special biochemical procedures are required to follow the elementary steps of the cleavage, and to obtain detailed information about the conformational changes of the interacting proteins. It was found by Goodno [1] that a complex of myosin with ADP and orthovanadate formed a stable structure, which allowed the studies on the conformation in this intermediate. Similar to vanadate, beryllium and aluminium fluorides also form stable

complexes with myosin in the presence of nucleotides [2,3]. It turned out that the stable complexes of ADP with vanadate, berylliofluoride and aluminofluoride bound to head of myosin mimic quite well the ATPase intermediates [4]. The atomic structure of truncated *Dictyostelium* subfragment 1 (S1) with BeF<sub>x</sub>, AlF<sub>4</sub> and V<sub>i</sub> was solved by Fisher et al. [5] and analysis of structures indicated that S1.ADP.BeF<sub>x</sub> complex resembled the M<sup>\*</sup>.ATP, whereas S1.ADP with AlF<sub>4</sub> mimics the AM.ADP.P<sub>i</sub> complex.

Differential scanning calorimeter (DSC) is a suitable method that directly monitors protein denaturation and unfolding, and the transition temperature  $T_m$  characterises the conformation stability [6–8]. In the present study we examined by DSC the complexes of myosin with actin in fibre system in the absence of nucleotides and the intermediate state of ATP hydrolysis by forming stable trapped complex with myosin and ADP and beryllium fluoride in muscle fibres. The comparison of the DSC results with other structural analogues of phosphate P<sub>i</sub> leads the conclusion that the AM.ADP.BeF<sub>x</sub> complex favours the AM.ADP.P<sub>i</sub> complex in fibre system.

\* Corresponding author. Tel.: +36 72 536 254; fax: +36 72 536 255.  
E-mail address: [timea.dergez@aok.pte.hu](mailto:timea.dergez@aok.pte.hu) (T. Dergez).

## 2. Materials and methods

### 2.1. Materials

Adenosine 5'-diphosphate (ADP), adenosine 5'-triphosphate (ATP), beryllium sulphate, ethylene glycol-bis( $\beta$ -aminoethyl ether)-*N,N'*-tetraacetic acid (EGTA), glycerol, histidine-HCl, magnesium chloride ( $\text{MgCl}_2$ ), potassium chloride (KCl) and sodium fluoride were obtained from Sigma (Germany).

### 2.2. Fibre preparation

Glycerol-extracted muscle fibre bundles were prepared from rabbit psoas muscle. Small stripes of muscle fibres were stored after osmotic shocks in 50% (v/v) glycerol, 80 mM KCl, 5 mM  $\text{MgCl}_2$ , 1 mM EGTA and 25 mM Tris-HCl, pH 7.0 at  $-18^\circ\text{C}$  up to one month. Fibre bundles from glycerinated muscle were washed for 60 min in rigor buffer (80 mM potassium propionate (KPr), 5 mM  $\text{MgCl}_2$ , 1 mM EGTA in 25 mM Tris-HCl buffer, pH 7.0) that removed glycerol, and then transferred to fresh buffer. Strong actin binding state (rigor), as well as weak actin binding transition state ( $\text{AM}\cdot\text{ADP}\cdot\text{P}_i$ ) was monitored.  $\text{AM}\cdot\text{ADP}\cdot\text{P}_i$  state was mimicked by addition of ATP and beryllium fluoride. Beryllium fluoride was prepared from 10 mM NaF and 3 mM  $\text{BeSO}_4$  immediately before experiments. Muscle fibres were stored in solution containing 80 mM KPr, 5 mM ATP, 5 mM  $\text{MgCl}_2$ , 1 mM EGTA in 25 mM Tris-HCl, pH 7.0 plus the corresponding chemicals for 15 min at  $0^\circ\text{C}$  and then DSC measurement was taken.

### 2.3. ATPase activity

The ATPase activity was determined using a pyruvate kinase-lactate dehydrogenase coupled optical test [9]. The assay medium for  $\text{Mg}^{2+}$ -ATPase consisted of 100 mM KCl, 20 mM MOPS, 1 mM  $\text{MgCl}_2$ , 0.5 mM EGTA, 0.15 mM NADH, 1 mM phosphoenol pyruvic acid, 20 U/ml pyruvate kinase, 40 U/ml lactic dehydrogenase, 0.5 mM ATP, pH 7.0. For  $\text{Ca}^{2+}$ - $\text{Mg}^{2+}$ -ATPase: assay medium plus 1 mM  $\text{CaCl}_2$ . At 340 nm the absorbance change was measured with a Perkin-Elmer spectrophotometer interfaced to a computer. The molar absorption coefficient of NADH was  $\epsilon(340\text{ nm}) = 6.22 \times 10^3 \text{ mol}^{-1} \text{ cm}^{-1}$ . In the experiments the  $\text{Mg}^{2+}$ -ATPase and the  $\text{Ca}^{2+}$ - $\text{Mg}^{2+}$ -ATPase activities of thin fibre bundles over 10 min intervals were determined. Fibre bundles of 8–10 mg wet weight were slightly stretched on a rectangular support made of platinum. The support was diagonally fitted into a standard quartz cuvette, which was filled in with the solutions. The solution was continuously mixed with a small magnetic bar. The decrease of fluorescence resulted in a straight line, the slope of the straight line was used to estimate the ATPase activity.

### 2.4. DSC technique

Thermal unfolding of muscle fibres in rigor and  $\text{ATP}\cdot\text{BeF}_x$  state was monitored by a SETARAM Micro DSC-II calorimeter. All experiments were conducted between 5 and  $80^\circ\text{C}$ , the

heating rate varied between 0.3 and 1.0 K/min in all cases. Conventional Hastelloy batch vessels were used during the denaturation experiments with 850  $\mu\text{L}$  sample volume (muscle fibres plus buffer) in average. Typical muscle wet weights for calorimetric experiments were between 200 and 250 mg. Rigor buffer was used as a reference sample. The sample and reference vessels were equilibrated with a precision of  $\pm 0.1$  mg. There was no need to do any correction between sample and reference vessels. The repeated scan of denatured sample was used as baseline reference, which was subtracted from the original DSC curve.

### 2.5. Evaluation of DSC measurements

In strong and weakly actin binding states the thermograms could be decomposed into three separate transitions in the main transition temperature range. Considering the muscle structure a fourth heat transition was also assumed which was assigned to actin. Deconvolution into four components was performed by using PeakFit 4.0 software from SPSS Corporation. For analysis of the single thermal transitions Gaussian functions were assumed. The comparison between the DSC patterns in different states of the fibre bundles suggested that the second and third Gaussian curves represented the myosin rod and the actin moiety. The third and second transition curves were subsequently subtracted from the main transition curve.

### 2.6. EPR measurements

Conventional EPR (electron paramagnetic resonance) spectra were taken with an ESP 300E (Bruker Biospin, Germany) spectrometer. First harmonic in-phase, absorption spectra were obtained by using 20 mW microwave power and 100 kHz field modulation with amplitude of 0.15 mT, the measurements were performed at temperature of  $23 \pm 1^\circ\text{C}$ . Spectra were normalised to the same number of unpaired electrons by calculating the double integral of the derived spectra.

## 3. Results and discussion

### 3.1. Evaluation of thermal transitions in muscle fibres

The reversibility of denaturation was checked by comparing the first scan of the muscle fibres with the second one after cooling the sample to room temperature. The DSC transitions were calorimetrically irreversible. The first DSC trace was corrected for the calorimetric base line by subtracting the second scan from the first one and for the difference in heat capacity by using a linear or sigmoidal base line. Figs. 1 and 2 show the DSC traces of muscle fibres in rigor and in  $\text{AM}\cdot\text{ADP}\cdot\text{BeF}_x$  intermediate states. The most striking feature of the traces that the transition temperature of the last peak strongly depends on the intermediate states of the muscle. Similar observations were obtained on isolated myosin subfragment 1 [10–13].

Systematic analysis of irreversible denaturation of protein systems started with the model by Lumry and Eyring [14]. After this basic report several experimental studies were reported with the conclusion, that, in many cases, the irreversible denaturation

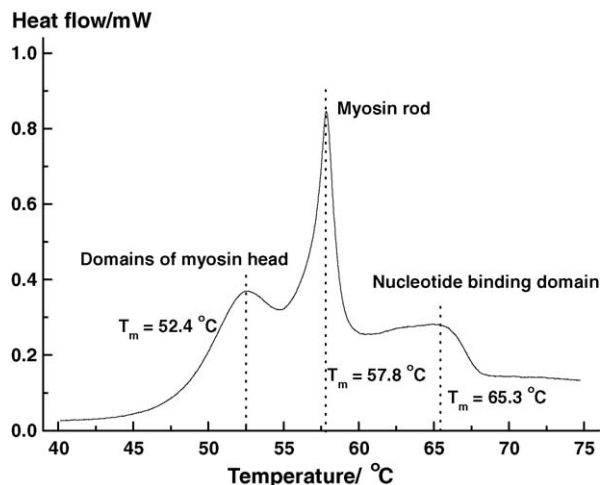


Fig. 1. DSC transition curves of muscle fibres in rigor. The baseline of the trace is not subtracted.

of proteins by DSC can be described on the basis of a simple two-state irreversible model [15–17]:



where N and F are the native and irreversibly denatured proteins, respectively. The  $k_{ap}$  reaction rate constant that governs the conversion from N to F is strongly temperature-dependent, first-order rate constant [18]. The theoretical analysis also suggests that the irreversible step from unfolded state to irreversible state is fast, and the amount of unfolded state is low [18].

The transition temperatures of the muscle fibres depended on scan rate, therefore it could be assumed that the melting of the muscle samples was determined by kinetic processes and could be described by the two-state kinetic model. It was shown later that at sufficiently high heating rates the thermodynamic equilibrium parameters could be extracted from the heat capacity curves [19]. We assumed Gaussian functions for the transition of the main proteins of the muscle fibres. The deconvolution

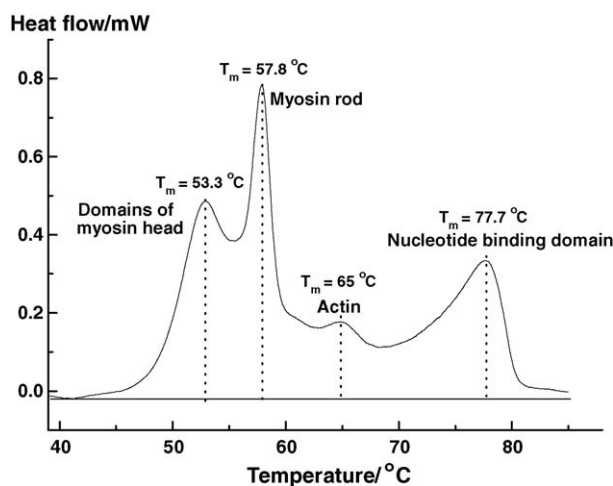


Fig. 2. Heat absorption curve obtained on muscle fibres in ADP.BeF<sub>x</sub> state. The transition temperatures of myosin domains are given.

resulted in four transitions, the first three transition temperatures were almost independent of the intermediate state of the muscle, the last transition temperature was shifted to higher temperature, when the buffer solution was manipulated to mimic the intermediate states of ATP hydrolysis (Figs. 1 and 2). The mean values for rigor were  $T_{m1} = 52.9 \pm 0.7$  °C,  $T_{m2} = 57.9 \pm 0.7$  °C,  $T_{m3} = 63.7 \pm 1.0$  °C. In order to obtain sufficient agreement with the experimental DSC trace, a fourth transition should be involved in the analysis. The second main protein that constitutes the striated muscle structure is actin. It represents some of 20% or more of the total protein in these cells, therefore it has significant contribution to the total heat absorption. Earlier experiments performed on globular and filamentous actin showed that the transition temperature of actin was in the range of 60–68 °C, depending of the state of actin [20–22].

The comparison of the main transitions for myosin and actin in solution and in fibres system shows significant increase of  $T_m$ , which is due to the interaction between actin and myosin in the filament structure. The stereospecific binding of the two myosin heads to actin induces a stabilisation at the head–tail junction and rod part of the myosin molecules in the thick filaments, that leads to decrease of cooperativity.

### 3.2. Effect of nucleotides on thermal transitions

The comparison between the DSC patterns in weakly binding states of myosin to actin, as in AM.ADP.P<sub>i</sub> or in AM.ADP.V<sub>i</sub> state, showed that the transition temperature at the second and third transitions (actin binding domain and myosin rod) varied only slightly, whereas the last one (the fourth transition) shifted markedly to higher temperature depending on the ternary complex. The last transition can be assigned to the nucleotide-binding domain of myosin. Its conformation open or closed depends on the bound nucleotide. In rigor and ADP state the conformation is open, whereas in the presence of ADP plus V<sub>i</sub> or BeF<sub>x</sub> the conformation is closed. This experimental conclusion was derived from analysis of X-ray diffraction data.

Addition of ADP plus BeF<sub>x</sub> to rigor buffer shifted the fourth transition to 77.7 °C, the highest value in weakly binding state of myosin to actin (Fig. 2). Successive subtraction of the transition of actin at  $T_m = 63.9$  °C and myosin rod at  $T_m = 57.7$  °C resulted in two asymmetric transitions (Fig. 3). According to earlier data [23] it can be accepted that the melting of subfragment 2 is also involved in the first endotherm transition, even in the case of muscle fibres. However, in the present state of our experiments we did not find any experimental fact how to resolve this trace into single transitions.

Biochemical and spectroscopic measurements suggest that the AM.ADP.BeF<sub>x</sub> state mimics the AM.ATP state, where the conformation of the nucleotide-binding domain is in closed state [24,25]. However, experiments performed on subfragment 1 of *Dictyostellium discoideum* showed that the open → closed transition depends on the temperature and the ionic strength [26]. Therefore, it can be suggested that the last transition is the superposition of two transitions; it expresses equilibrium between open and closed states. The changes in the thermal transitions induced by nucleotides stem in part from conforma-

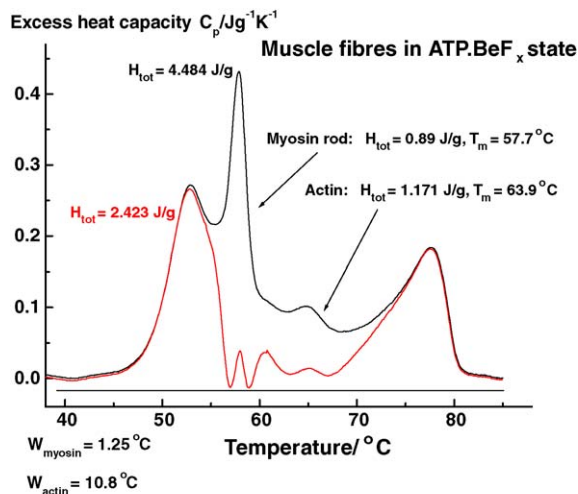


Fig. 3. Excess heat capacity curve of the intermediate state  $\text{ADP.BeF}_x$ . The melting curves of myosin rod and actin filaments were subtracted from the complex DSC transition. The line widths at half-height, the location and the contribution of the single transitions were varied.

tional changes of the globular motor portion and from protein interactions between actin and myosin [27,28]. Further possible interpretation might be that the structure of the ternary complex differs in dimensional asymmetry and/or in internal flexibility. Fluorescence measurements showed that the distance between  $\epsilon\text{ADP}$  and SH1 is shorter in S1- $\epsilon\text{ADP-V}_i$  complex, but this distance is unperturbed in acto-S1- $\epsilon\text{ADP-V}_i$  complex [29]. Comparison with various nucleotide-bound S1 complexes indicates that the shape of S1 in S1-ADP and S1-ADP- $P_i$  states significantly differs from the shape of S1 in nucleotide-free states [30].

The sum of the areas under the first and last curves was practically constant, but their fractions depended on the state of the muscle. In strongly binding state of myosin to actin (rigor, ADP state) the fraction of the first transition was much larger, than the last one, whereas in weakly binding state of myosin to actin, the fraction of the first transition decreased at the expense of the last one. It supports also the view that these transitions are parts of the same portion of the myosin molecule.

### 3.3. EPR results

In order to obtain information about the conformational changes that occur in the muscle structure in the presence of nucleotides and find correlation with the DSC results, EPR experiments were performed on fibre bundles. The reactive Cys 707 residue of myosin heads was spin-labelled with isothiocyanate probe molecules as described earlier [31]. Fig. 4 shows the EPR spectra obtained on fibre bundles, the long axis of the fibres was oriented parallel to the laboratory magnetic field. It known from earlier studies that myosin heads have stereospecific orientation in the absence of nucleotides and in the presence of ADP (upper spectra), but the addition of ATP and  $\text{AlF}_3$  induce an order-to-disorder transition of myosin heads (bottom spectrum [32,33]). In this state the myosin heads are dynamically disordered, and the orientation dependence of EPR spectra disap-

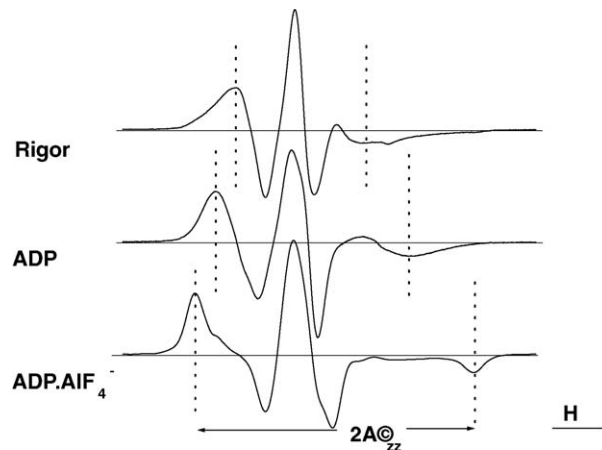


Fig. 4. EPR spectra of spin-labelled myosin heads in muscle fibre bundles in rigor, ADP and  $\text{ADP.AlF}_4^-$  state. The distance between the dotted lines shows the hyperfine coupling constant. The drastic change of line shape in  $\text{ADP.AlF}_4^-$  state represents the disorder of the myosin heads induced by  $\text{ADP.AlF}_4^-$ .

pears. The hyperfine coupling constant  $2A'_{zz}$  is exactly the same as in the case of randomly oriented fibres ( $2A'_{zz} = 6.785$  mT). Myosin rod and the regulation domain are little affected by nucleotides and nucleotide analogues in striated muscle.

Therefore, it can be suggested that the large conformational change of myosin heads induced by ATP and inorganic phosphate analogue  $\text{AlF}_3$  might be responsible for the significant change of the DSC pattern. In the case of ADP only a moderate effect is expected, as derived from both DSC and EPR measurements as well. However, it cannot be excluded that the second large protein component actin can also contribute to the shape of the heat transition curve.

### Acknowledgement

The SETARAM Micro DSC-II used in the experiments was purchased with fund provided by the National Research Foundation Grant CO-272.

### References

- [1] C.C. Goodno, Proc. Natl. Acad. Sci. U.S.A. 76 (1979) 2620.
- [2] B.C. Phan, E. Reisler, Biochemistry 31 (1992) 4787.
- [3] S. Maruta, G.D. Henry, B.D. Snykes, M. Ikebe, J. Biol. Chem. 268 (1993) 7093.
- [4] M.M. Werber, Y.M. Peyser, A. Muhrad, Biochemistry 31 (1992) 7190.
- [5] A.J. Fisher, C.A. Smith, J. Thoden, R. Smith, K. Sutoh, H.M. Holden, I. Rayment, Biochemistry 34 (1995) 8960.
- [6] D. Lőrinczy, J. Belágyi, Thermochim. Acta 296 (1997) 161.
- [7] D. Lőrinczy, J. Belágyi, Thermochim. Acta 343 (2000) 27.
- [8] D. Lőrinczy, J. Belágyi, Eur. J. Biochem. 268 (2001) 5970.
- [9] D.R. Trentham, R.G. Bardsley, J.P. Eccleston, A.G. Weeds, Biochem. J. 126 (1972) 635.
- [10] D.I. Levitsky, V.L. Shnyrov, N.V. Khvorov, A.E. Bukatina, N.S. Vedenkina, E.A. Permyakov, O.P. Nikolaeva, B.F. Poglazov, Eur. J. Biochem. 209 (1992) 829.
- [11] A.A. Bobkov, N.K. Khvorov, N.L. Golitsina, D.I. Levitsky, FEBS Lett. 332 (1993) 64.
- [12] N.L. Golitsina, A.A. Bobkov, I.V. Dedova, D.A. Pavlov, O.P. Nikolaeva, V.N. Orlov, D.I. Levitsky, J. Muscle Res. Cell Motil. 17 (1996) 475.

- [13] D. Lőrinczy, J. Belágyi, *Biochem. Biophys. Res. Commun.* 217 (1995) 592.
- [14] R. Lumry, H. Eyring, *J. Phys. Chem.* 58 (1954) 110.
- [15] J.M. Sanchez-Ruiz, J.L. Lopez-Lacomba, M. Cortijo, P.L. Mateo, *Biochemistry* 27 (1988) 1648.
- [16] F. Conjero-Lara, P.L. Mateo, F.X. Aviles, J.M. Sanchez-Ruiz, *Biochemistry* 30 (1991) 2067.
- [17] M. Thorolfson, B. Ibarra-Molero, P. Fojan, S.B. Petersen, J.M. Sanchez-Ruiz, A. Martinez, *Biochemistry* 41 (2002) 7573.
- [18] I.M. Plaza del Pino, B. Ibarra-Molero, J.M. Sanchez-Ruiz, *Proteins Struct. Funct. Genet.* 40 (2000) 58.
- [19] T. Vogl, C. Jatzke, H.-J. Hinz, J. Benz, R. Huber, *Biochemistry* 36 (1997) 1657.
- [20] D. Lőrinczy, J. Belágyi, *Thermochim. Acta* 259 (1995) 153.
- [21] B. Visegrády, D. Lőrinczy, G. Hild, B. Somogyi, M. Nyitrai, *FEBS Lett.* 565 (2004) 163.
- [22] B. Visegrády, D. Lőrinczy, G. Hild, B. Somogyi, M. Nyitrai, *FEBS Lett.* 579 (2005) 6.
- [23] D. Lőrinczy, N. Hartvig, J. Belágyi, *J. Biochem. Biophys. Meth.* 53 (2002) 75.
- [24] M.A. Geeves, K.C. Holmes, *Annu. Rev. Biochem.* 68 (1999) 687.
- [25] E. Pate, N. Naber, M. Matuska, K. Franks-Skiba, R. Cooke, *Biochemistry* 36 (1997) 12155.
- [26] K. Ajtai, M. Peyser, S. Park, T.P. Burghardt, A. Muhlrads, *Biochemistry* 38 (1999) 6428.
- [27] S. Highsmith, D. Eden, *Biochemistry* 29 (1990) 4087.
- [28] R. Aguirre, S.-H. Lin, F. Gonsolin, C.-H. Wang, C.H. Cheung, *Biochemistry* 28 (1989) 799.
- [29] D.I. Levitsky, N.V. Khovorov, V.L. Shnyrov, N.S. Vedenkina, E.A. Permyakov, B.F. Poglazov, *FEBS Lett.* 264 (1990) 176.
- [30] S. Highsmith, K. Polosukhina, D. Eden, *Biochemistry* 39 (2000) 12330.
- [31] J. Belágyi, I. Frey, L. Pótó, *Eur. J. Biochem.* 224 (1994) 215.
- [32] P.G. Fajer, E.A. Fajer, M. Schoenberg, D.D. Thomas, *Biophys. J.* 60 (1991) 642.
- [33] N. Hartvig, D. Lőrinczy, N. Farkas, J. Belágyi, *Eur. J. Biochem.* 269 (2002) 2168.